Novel Permanent-Magnet-Biased Axial Hybrid Magnetic Bearings without a Thrust Disc

Pengfei Zhang, Zhiheng Wang, Guang Xi

School of Energy and Power Engineering, Xi'an Jiaotong University
28 Xianning West Road, 710049, Xi'an, P.R. China
pfzhang1234@gmail.com, wangzhiheng@mail.xjtu.edu.cn, xiguang@mail.xjtu.edu.cn

***Abstract*—The paper proposes a pair of novel permanent-magnet-biased axial hybrid magnetic bearings, which are assembled at ends of a compressor spindle. The outer diameter of rotor is minimized to reduce the wind loss, which is regarded as the main loss in a typical axial magnetic bearing for a compressor. The bias magnetic flux, provided by an axial polarized permanent magnet ring, diminishes the loss further. The paper firstly introduces the structure and the working principle of the new axial hybrid magnetic bearing system. The cooling holes are aimed to improving the cooling capability without degrading the load capacity. Then, the axial magnetic attraction forces of axial magnetic bearings in pairs, under the condition without the cooling holes, are calculated by 2-D Finite Element Method (FEM) and 3-D FEM respectively. Additionally, another 3-D model is set up to investigate the influence of the designed cooling holes on the axial force. The coupling of the magnetic force and the flux density limit of iron cores are analyzed. The numerical results indicate that the proposed structure of the axial magnetic bearing system is feasible.**

I. INTRODUCTION

Magnetic bearings have been applied to high-speed turbomachinery progressively for their advantages such as noncontact, no lubrication requirement, lower power loss and less maintenance [1-3]. Compared with active magnetic bearings, permanent-magnet-biased hybrid magnetic bearings further reduce the power loss by generating the bias magnetic field instead of the current in coils [4].

Although much attention has been focused on the new design of permanent-magnet-biased radial and radial-axial magnetic bearings, quite few studies have been performed on the new structures of permanent-magnet-biased axial hybrid magnetic bearings. Khoo et al. [5] proposed a high load capacity bearing that generates the force from a number of parallel stator and rotor discs. Fang et al. [6] suggested a novel 3-DOF axial hybrid magnetic bearing, which is used in reaction flywheel system. The iron loss of magnetic bearing is reduced through a parallel-slot structure. A new structure of permanent-magnet-biased axial hybrid magnetic bearings was described in [7]. The power loss is diminished by separating the path of bias flux and control flux. However, all of those axial magnetic bearings mentioned above have an obvious thrust disc, which leads to a maximum material strain increase and larger rotor unbalances [8]. Moreover, in case of a rotor running in the air or other gases, the gas friction loss increases sharply with the increase of the outer diameter of a thrust disc [9]. Due to the high pressure condition in turbomachinery, the gas friction loss caused by fluid turbulence is the main power loss of magnetic bearings. A tubular linear actuator without a thrust disc was employed as a permanent-magnet-biased axial hybrid magnetic bearing in literature [8]. However, the axial load capacity is limited.

To overcome these drawbacks of the existing axial magnetic bearings, especially the high gas friction loss, a new structure of permanent-magnet-biased axial hybrid magnetic bearing system is proposed in this paper. Firstly its working principle is introduced. The characteristics of the magnetic force are analyzed based on 2-D FEM and 3-D FEM respectively. A 3-D Finite Element Analysis (FEA) is conducted to study the feasibility of the cooling holes design. In addition, the coupling of the force between axial direction and radial direction and saturation flux density limit are also analyzed by the 3-D FEM.

II. PRINCIPLE OF PERMANENT-MAGNET-BIASED AXIAL MAGNETIC BEARING SYSTEM

The configuration of the new axial magnetic bearing system is shown in Figure 1, which is assembled at both ends of a compressor spindle. The new system consists of the rotor, the stator, the working gaps and the cooling holes. The rotor includes an upper end plate, a spindle and a bottom end plate. The spindle is along the Z-axis of cylindrical coordinates. The stator has two parts, i.e., the upper stator and the bottom stator, each of which has an inner housing, a spacer, coils, a hood, a permanent magnet ring and an outer housing. The working gaps are named according to their location, that is, the working gap between the inner housing and the end plate is

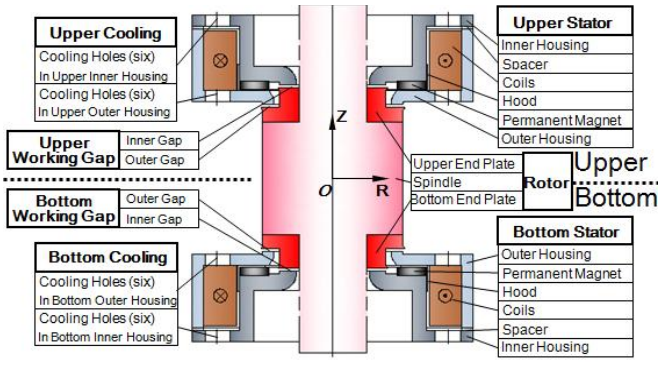

Figure 1. Permanent-magnet-biased axial hybrid magnetic bearing system.

named as the inner gap, while that between the outer housing and the end plate is called by the outer gap. Both the upper and bottom axial magnetic bearings have an inner gap and an outer gap, which together are named as upper working gap and bottom working gap respectively.

Figure 2 shows the magnetic flux schematic diagram in the half section of the bottom bearing. The magnetic flux is classified into the bias magnetic flux and the control magnetic flux. The dotted lines with the hollow arrows denote the flux paths generated by the permanent magnet and the solid lines with the solid arrows denote the flux paths generated by the coil. The flux provided by the permanent magnet is separated into two paths: One is the bias flux flowing across the inner housing, the inner gap, the end plate, the outer gap, the outer housing and the hood, and the other is the flux through the inner housing, the spacer, the outer housing and the hood. The control flux generated from the coil with the current flows across the inner housing, the inner gap, the end plate and the outer housing. Based on the working gap, the attractive magnetic force on the rotor is generated by the bias magnetic flux and control magnetic flux flowing through them. The spacer is inserted to guarantee that enough magnetic flux goes through the working gap, and the permanent magnet is thick enough to ensure the main control flux goes through the working gap other than through the permanent magnet. Therefore, the control flux circuits are of low reluctance, and the new axial magnetic bearing system is of low loss.

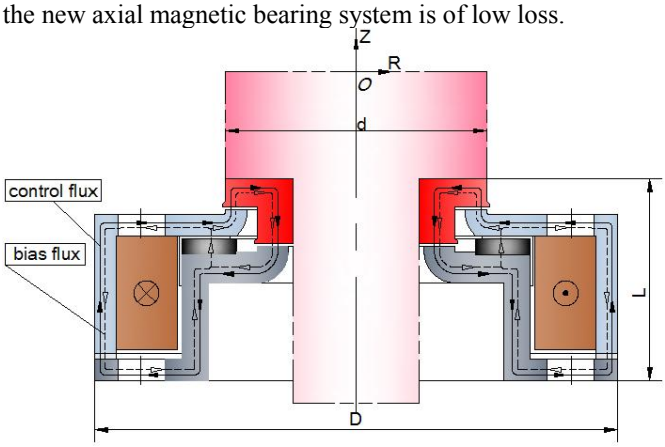

Figure 2. Schematic diagram of the bottom bearing system.

Assuming that the rotor is disturbed along positive Z-axis direction without loss of generality, it will move to positive Z-axis direction under the attractive magnetic force. As a result of the motion, the bottom working gap of the axial magnetic bearing gets larger, while the upper working gap gets smaller. The displacement sensors sense this motion and transmit it to the control system, and then the control system sends an amplified control current through the corresponding coils. The process results in the additional control flux of the bottom bearing denoted by the solid lines with the solid arrows in Figure 2, which is controlled by the controller to pull the rotor back to the equilibrium position. If the direction of current in coils is shown as Figure 1 and the magnetization of the upper magnetic ring is opposite to that of the bottom magnetic ring, the control flux direction of the upper bearing is the same as that of the bottom one. However, the bias flux direction is opposite between them. Thus, the bias flux in the upper working gap is reduced by the corresponding control flux, while the bias flux in the bottom working gap is increased by the corresponding control flux. By adding the flux in the bottom (i.e., larger) working gap and subtracting the flux in the upper (i.e., smaller) working gap, the axial magnetic bearing system generates an axial restoring force to stable the rotor.

The cooling holes on the inner housing and the outer housing are designed to improve the cooling capability without the degradation of magnetic force. It is guaranteed by the sectional area that the flux goes across is no less than that of magnetic poles, especially where cooling holes locate. The R coordinates of cylindrical holes' center here are the same, so cooling fluid could flow through the cavity between the inner and outer housing directly.

III. FINITE ELEMENT ANALYSIS

A. Models and Parameters

The main parameters of the proposed axial magnetic bearing system are listed in Table I. The working gap length, δ_i and δ_0 , is 0.3mm recommended by ISO standard [10], while the pole area A_i and A_o is nearly equivalent to increase the axial load capability as much as possible. The values of d and D are set based on the compressor. L, shown in Figure 2, is designed for enough volume of coils. The parameters, δ_h and δ_s, are set to adjust the bias flux in working gaps without reducing the control flux too much. Cooling holes' diameter d_h is maximized to improve the cooling capability with no impact on the magnetic force characteristics.

To verify the feasibility of the new structure, the proposed axial magnetic bearing system is analyzed by FEM with ANSYS Maxwell Software. The 2-D FEM and 3-D FEM analysis models were built as shown in Figures 3 and 4 respectively. As shown in Figure 3(a), a symmetrical configuration of bearings in pairs was built for the simulation. Since the axial bearing system is axisymmetric, the 2-D FEM can solve the steady problem with suitable boundary conditions. Figure 3(b) shows the whole mesh of the model above. In Figure 3(c), it's obvious that finite element refinement has been conducted in the working gap. For 2-D FEM analysis, the model is axisymmetric about Z-axis and is without cooling holes. However, for 3-D FEM analysis, the rotor in Figure 4(a) may be misaligned in order to study the force coupling between Z direction and R direction. Figure 4(b) shows the 3-D model with cooling holes. It was built to validate that the cooling holes have little influence on the force characteristics of this magnetic bearing system.

TABLE I. PARAMETERS OF THE AXIAL MAGNETIC BEARING SYSTEM

	Parameter	Value
d	Outer rotor diameter	50 mm
D	Outer stator diameter	100 mm
L	Axial length	38.5 mm
δ_i	Inner gap length	0.3 mm
δ_o	Outer gap length	0.3 mm
δ_s	Thickness of spacer	1.1 mm
δ_h	Thickness of hood bottom	0.7 mm
A_i	Pole area of inner housing	591.28 mm^2
A_o	Pole area of outer housing	591.22 mm^2

	Parameter	Value
h_{pm}	Thickness of permanent magnet	3 mm
N	Turns of coils	300
d_h	Cooling holes' diameter	9.6 mm
B_s	Saturation flux density of iron core	1.5 T

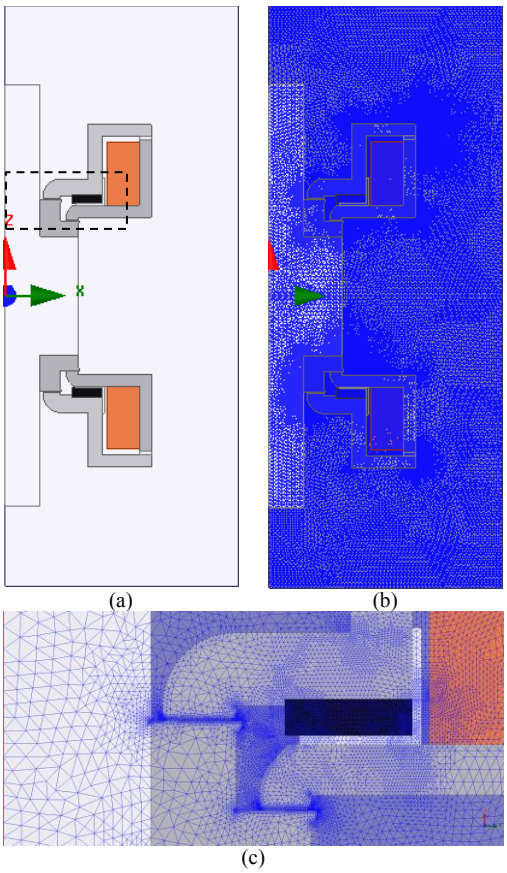

Figure 3. The 2-D FEM model and final mesh of the axial magnetic bearing system. (a) The 2-D FEM model of the axial magnetic bearing system. (b) The whole mesh of 2-D FEM model. (c) The local mesh in box of (a).

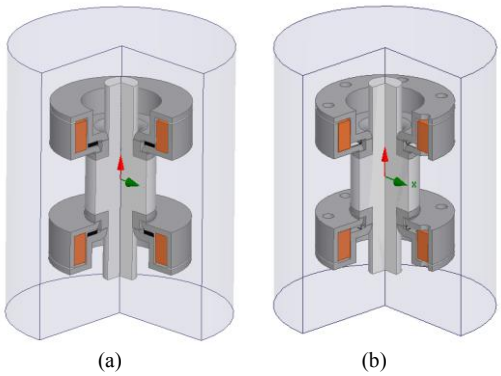

Figure 4. The 3-D FEM model of the axial magnetic bearing system. (a) The 3-D FEM model without cooling holes. (b) The 3-D FEM model with cooling holes.

B. *Boundary and Excitation*

The external boundaries are set as "balloon". The nonlinearity of iron cores is concerned and the magnetization direction of permanent magnet at the top is opposite to that at the bottom which pointing to +Z direction. For the upper coils and the bottom coils, their current sources are equal and share the same direction. As shown in Figure 1, the current in coils is assumed to be positive, and it will generate the negative force, pointing to –Z direction.

IV. Simulation Results and Analysis

A. *Basic Characteristics*

The force-displacement and force-current relationships are the main features of magnetic bearing. By 2-D FEM and 3-D FEM, they are displayed in Figure 5.The models are built without the cooling holes. The simulation results show that the results by 2-D FEM are generally consistent with the results by 3-D FEM. Figure 5(a) shows the proposed permanent-magnet-bias axial magnetic bearing system has a nearly linear force-current characteristic at whole range of current in coils, especially in 3-D FEM analysis. In addition, from Figure 5(b), the force-current characteristic is nearly linear when the displacement of rotor is less than 10^{-4} m in Z direction. Except the condition that the rotor displacement is zero, the force-displacement factor from 2-D FEA is larger than that from 3-D FEA. The force error between them increases if the rotor departures its equilibrium position.

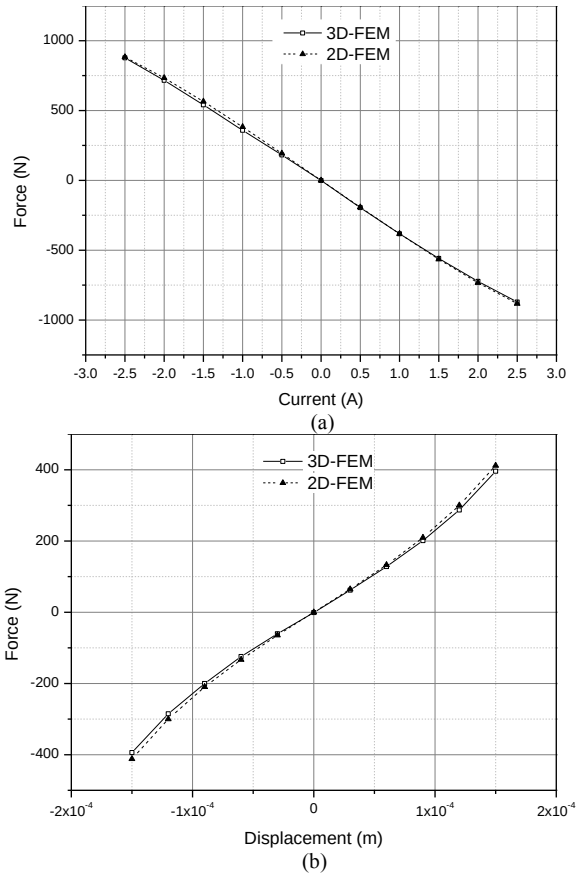

Figure 5. Force-displacement and force-current characteristic of the axial magnetic bearing system. (a) Axial force variation with current. (b) Axial force variation with displacement.

B. Cooling Holes' Influence

The force performances of the presented magnetic bearings with and without cooling holes are compared in Figure 6, which illustrates that their deviations are very small at all the range of current and displacement. That indicates the cooling holes have little influence on the force-displacement and force-current relationships. However, the holes in the bearings can greatly contribute to heat dissipation of coils in working gas.

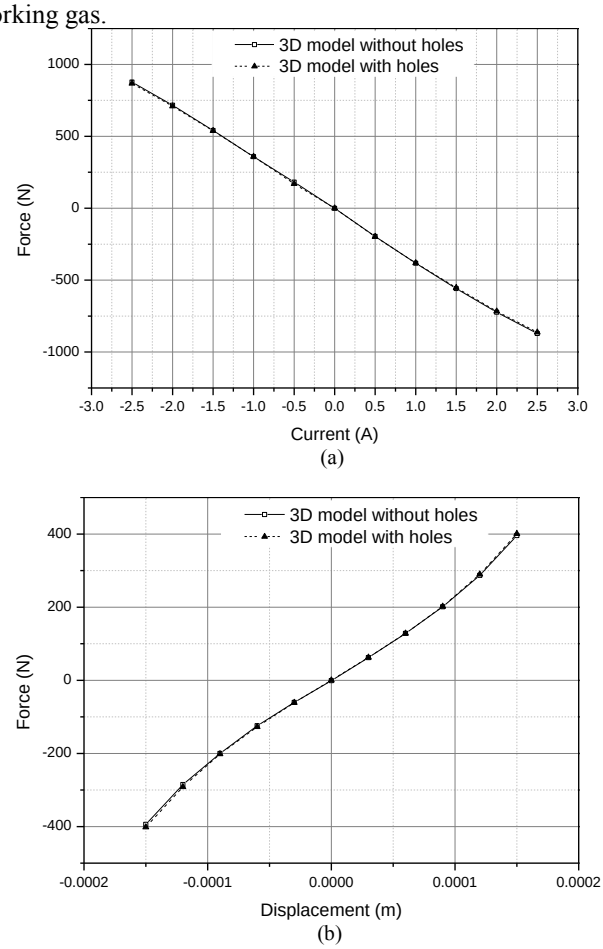

Figure 6. Influence of cooling holes on mechanical property. (a) Axial force variation with current. (b) Axial force variation with displacement.

C. Coupling with R Direction

Since the translation of the rotor along R direction is limited to 0.15mm, i.e., the nominal gap of radial back-up bearings will be employed as 0.15mm, the axial force variation with the displacement and the current is calculated by 3-D FEM with the assumption that the rotor translates 0.15mm along positive X-axis. In this section, the model analyzed is with the cooling holes. In Figure 7, it can be found that the force-current curves, as well as the force-displacement curves, are almost overlapped. Therefore, the motion effect on the axial force is small.

Figures 8 (a) & (b) depict the force variation along X-axis (i.e. F_x). In Figure 8(a), without the rotor motion, the forces deviate from zero due to the numerical simulation error. However, with the rotor motion, the forces reduce and are negative, except the condition that the current is zero. The larger the current is, the more the corresponding force reduction will be. But it should be further studied that whether it is a restoring force which may stable the rotor, or it is just caused by the numerical error. According to the results when x = 0.0mm, the numerical error is about 0.1N. Therefore, it seems that it could be a restoring force except the situation that the current is 0A. Here, the maximum value of F_x is less than 0.7N, so the influence of the rotor motion along X-axis can be ignored or be regarded as a small disturbance.

It can be seen from Figure 8(b) that, without rotor motion, the maximum force deviation from zero is about 0.1N, while with the rotor motion, it is about 0.15N. Both of them are quite small. So, the variation of force caused by rotor motion is very small, and the force variation can also be ignored.

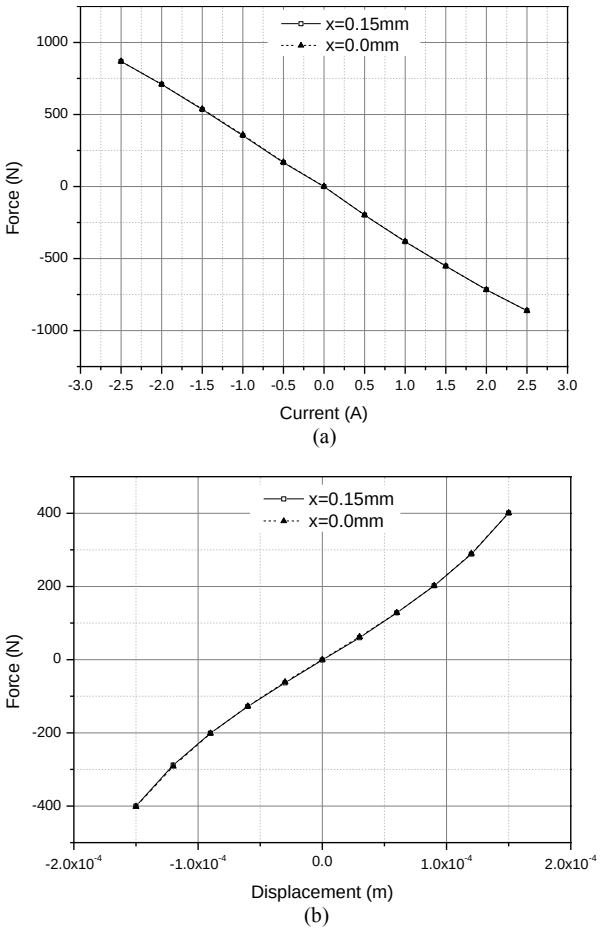

Figure 7. Comparison of mechanical property on rotor motion along X-axis. (a) Aixal force variation with current. (b) Aixal force variation with displacement.

D. Flux Density Limit of Iron Core

The maximum load capability is expressed as Equation (1):

$$F = \frac{B_s^{\,2} A}{\mu_0} \tag{1}$$

where B_s is the saturation flux density, A denotes the total area of magnetic poles, and μ_0 is the permeability of free space. Figure 9 shows the flux density distribution at the axial sectional view, which only displays that in the components (i.e., the background distribution doesn't display here.)

The rotor is at the equilibrium position, and the current in coils is 2.0A in Figure 8(a) and 2.5A in Figure 8(b). The flux density in parts of inner housing and outer housing is more than saturation flux density of iron cores, 1.5T, as shown in circles of Figures 8(a) & (b). The area where flux density is no less than 1.5T gets larger, if the current in coils gets bigger. Nevertheless, the force-current factor is almost constant, which is plotted in Figure 6(a) and Figure 7(a).

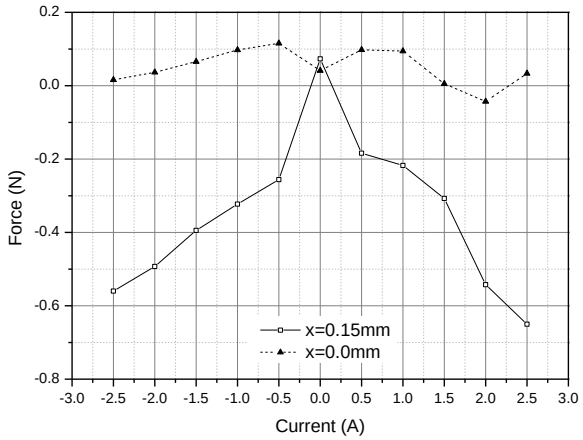

(a)

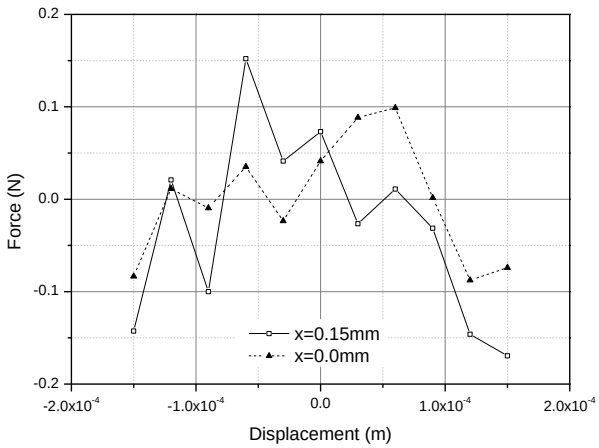

(b)

Figure 8. Force along X-axis under the influence of rotor motion. (a) F_x variation with current. (b) F_x variation with displacement.

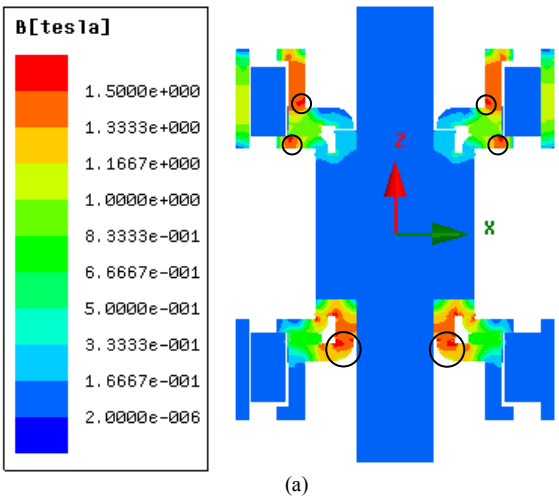

(a)

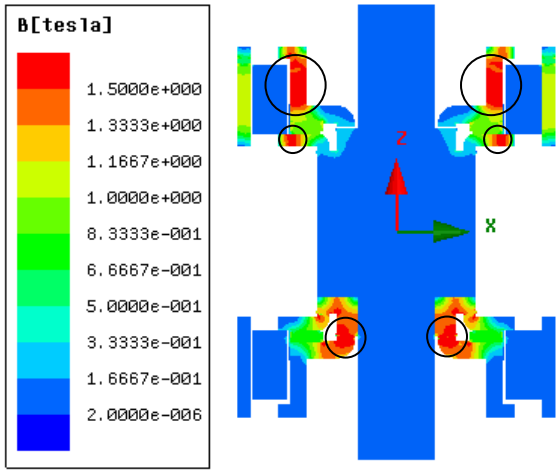

(b)

Figure 9. Flux density distribution at the axial sectional view. (a) Current =2.0A. (b) Current =2.5A.

V. CONCLUSIONS

A new structure of a permanent-magnet-biased axial magnetic bearing system without a thrust disc has been proposed to reduce the power loss, especially the gas friction loss, and to improve the cooling capability without the degradation of load capability. According to the results by 2-D FEM and 3-D FEM, we could make conclusions as follows:

- The proposed axial magnetic bearing system has a linear force-current factor and a force-displacement factor if the current in coils is no more than 2.5A and the displacement of rotor is less than 10^{-4} m.
- The designed cooling holes have little influence on the force characteristics, but it will contribute to improve the heat dissipation by convection.
- The effect of rotor motion along R direction on axial force is small, and the effect on radial force can also be ignored. It indicates that the axial force produced by the magnetic bearing system decouples with the radial force.
- Under the large current conditions, the flux density is saturate in some area. In spite of the flux density limit of iron cores, the axial force is still proportional to the current in coils.

It can be concluded that the presented structure of the axial magnetic bearing is feasible. It is interesting that the radial force by the current in coils seems to stable the rotor in corresponding radial direction, even though it's quite small. In future, the phenomenon will be further investigated, and the experiments will be conducted.

ACKNOWLEDGMENT

This present work is financially supported by the National Nature Science Foundation of China under grant No. 51236006.

REFERENCES

[1] J. Schmied. "Experience with magnetic bearings supporting a pipeline compressor," *Proceedings of 2nd Int. Symp. On Magnetic Bearings*, pp. 47–55, 1990.

[2] W. Canders, N. Ueffing, U. Schrader-Hausmann, R. Larsonneur, "MTG400:A magnetically levitated 400 KW turbo generator system for

natural gas expansion," *Proceedings of 4th Int. Symp. on Magnetic Bearings*, pp. 435–440, 1994.
[3] S. Yu, G. Yang, L. Shi, Y. Xu, "Application and research of the active magnetic bearing in the nuclear power plant of high temperature reactor", *Proceedings of 10th Int. Symp. On Magnetic Bearings*, pp. 1–7,2006.
[4] A. C. Lee, F. Z. Hsiao, D. Ko, "Analysis and testing of magnetic bearing with permanent magnets for bias," *JSME International Journal*, vol. 37, no. 3, pp. 774–782, 1994.
[5] W. K. S. Khoo, K. Kalita, S. D. Garvey, R. J. Hill-Cottingham, J. F. Eastham, "Active axial-magnetomotive force parallel-airgap serial flux magnetic bearings," *IEEE Transactions on Magnetics*, vol. 46, no. 7, pp. 2596–2602, 2010.
[6] J. Fang, J. Sun, H. Liu, J. Tang, "A novel 3-DOF axial hybrid magnetic bearing," *IEEE Transactions on Magnetics*, vol. 46, no. 12, pp. 4034-4045, 2010.
[7] J. Fang, J. Sun, Y. Xu, X. Wang, "A new structure for permanent-magnet-biased axial hybrid magnetic bearings," *IEEE Transactions on Magnetics*, vol. 45, no. 12, pp. 5319-5325, 2009.
[8] C. Weißbacher, H. Stelzer, K. Hameyer, "Application of a tubular linear actuator as an axial magnetic bearing," *IEEE/ASME Transactions on Mechatronics*, vol. 15, no. 4, pp. 615–622, 2010.
[9] Mack, M., "Luftreibungsverluste bei elektrischen Maschinen kleiner Baugröße," Diss. TH Stuttgart, 1967.
[10] ISO Standard 14839-4, Mechanical vibration - Vibrations of rotating machinery equipped with active magnetic bearings - Part 4: Technical guidelines, 2012.